Epidermal hepcidin is required for neutrophil response to bacterial infection

Malerba, Mariangela ; Louis, Sabine ; Cuvellier, Sylvain ; Mairpady Shambat, Srikanth ; Hua, Camille ; Gomart, Camille ; Fouet, Agnès ; Ortonne, Nicolas ; Decousser, Jean-Winoc ; Zinkernagel, Annelies S ; Mathieu, Jacques R R ; Peyssonnaux, Carole

Abstract: Novel approaches for adjunctive therapy are urgently needed for infections complicated by antibiotic-resistant pathogens and for patients with compromised immunity. Necrotizing fasciitis (NF) is a destructive skin and soft tissue infection. Despite treatment with systemic antibiotics and radical debridement of necrotic tissue, lethality remains high. The key iron regulatory hormone hepcidin was originally identified as a cationic antimicrobial peptide (AMP), but its putative expression and role in the skin, a major site of AMP production, has never been investigated. We report here that hepcidin production is induced in the skin of patients with Group A Streptococcal (GAS) NF. In a GAS-induced NF model, mice lacking hepcidin in keratinocytes failed to restrict systemic spread of infection from an initial tissue focus. Unexpectedly, this effect was due its ability to promote production of the CXCL1 chemokine by keratinocytes resulting in neutrophil recruitment. Unlike CXCL1, hepcidin is resistant to degradation by major GAS proteases and could therefore serve as a reservoir to maintain steady state levels of CXCL1 in infected tissue. Finally, injection of synthetic hepcidin at the site of infection can limit or completely prevent systemic spread of GAS infection suggesting that hepcidin agonists could have a therapeutic role in NF.

DOI: https://doi.org/10.1172/JCI126645

JCI The Journal of Clinical Investigation

Epidermal hepcidin is required for neutrophil response to bacterial infection

Mariangela Malerba, … , Jacques R.R. Mathieu, Carole Peyssonnaux

J Clin Invest. 2019. https://doi.org/10.1172/JCI126645.

Concise Communication In-Press Preview Infectious disease

Graphical abstract

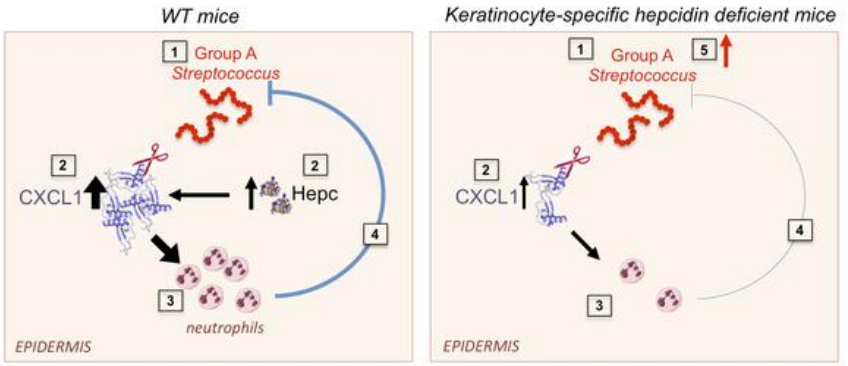

Epidermal hepcidin is required for neutrophil response to bacterial infection

Mariangela Malerba[1,2] , Sabine Louis[1,2], Sylvain Cuvellier[1,2], Srikanth Mairpady Shambat[3], Camille Hua[4], Camille Gomart[5], Agnès Fouet[1,] , Nicolas Ortonne[6], Jean-Winoc Decousser[5], Annelies S Zinkernagel[3], Jacques RR Mathieu[1,2,#], Carole Peyssonnaux[1,2,#,*]

[1] Université de Paris, Institut Cochin, INSERM, U1016, CNRS, UMR8104, F-75014 PARIS, France

[2] Laboratory of Excellence GR-Ex, Paris, France

[3] Department of Infectious Diseases and Hospital Epidemiology, University Hospital Zurich, University of Zurich, Zurich, Switzerland

[4]Assistance Publique-Hôpitaux de Paris, Service de dermatologie, Hôpital Henri Mondor, Créteil, France, Université Paris Est Creteil EA 7379 EPiderME

[5] Assistance Publique-Hôpitaux de Paris, Hôpitaux Universitaires Henri Mondor, Laboratoire de Bactériologie Hygiène et Equipe Opérationnelle d'Hygiène EA 7380 Dynamyc Université Paris-Est Créteil (UPEC), Ecole nationale vétérinaire d'Alfort (EnvA), Faculté de Médecine de Créteil, Créteil, France.

[6] Pathology department, APHP, Henri Mondor hospital, UPEC university and INSERM U955, team 9

*** Corresponding author:**

Carole Peyssonnaux, PhD

Institut Cochin, Department Endocrinology Metabolism and Diabetes

INSERM U1016, CNRS UMR8104

24 rue du Faubourg Saint Jacques

75014 Paris, FRANCE

e-mail : carole.peyssonnaux@inserm.fr

Phone : (33)1 44 41 24 71

Fax : (33)1 44 41 24 21

co-last authorship

The authors have declared that no conflict of interest exists.

International Patent Application N° PCT/IB2018/000884 filed May, 4 2018 entitled « Methods for treating gram positive bacterial infection » in the name of Inserm, CNRS, Université Paris Descartes. Inventors Mariangela Malerba, Jacques Mathieu, Carole Peyssonnaux

Abstract

Novel approaches for adjunctive therapy are urgently needed for infections complicated by antibiotic-resistant pathogens and for patients with compromised immunity. Necrotizing fasciitis (NF) is a destructive skin and soft tissue infection. Despite treatment with systemic antibiotics and radical debridement of necrotic tissue, lethality remains high. The key iron regulatory hormone hepcidin was originally identified as a cationic antimicrobial peptide (AMP), but its putative expression and role in the skin, a major site of AMP production, has never been investigated. We report here that hepcidin production is induced in the skin of patients with Group A Streptococcal (GAS) NF. In a GAS-induced NF model, mice lacking hepcidin in keratinocytes failed to restrict systemic spread of infection from an initial tissue focus. Unexpectedly, this effect was due its ability to promote production of the CXCL1 chemokine by keratinocytes resulting in neutrophil recruitment. Unlike CXCL1, hepcidin is resistant to degradation by major GAS proteases and could therefore serve as a reservoir to maintain steady state levels of CXCL1 in infected tissue. Finally, injection of synthetic hepcidin at the site of infection can limit or completely prevent systemic spread of GAS infection suggesting that hepcidin agonists could have a therapeutic role in NF.

Introduction

Necrotizing Fasciitis (NF) is an infection characterized by widespread necrosis of the skin, subcutaneous tissues and fascia that was first described by Hippocrates in the 5th century (1). The standard treatment of NF consists of broad-spectrum antibiotics, extensive surgical debridement, and supportive care. However, even with current state-of-the-art treatment, NF frequently takes a fulminant course and is still associated with high mortality rates up to 35% (1). Group A *Streptococcus* (GAS) is considered the most common cause of NF associated with bacteremia and shock. Upon detection of these Gram-positive pyogenic bacteria, neutrophil recruitment is critical to the resolution of infection (2). However, GAS is equipped with a magnitude of virulence factors allowing the pathogen to uniquely counteract each anti-bacterial strategy of neutrophils (3).

Hepcidin was originally identified as a cationic antimicrobial peptide (AMP) by its close structural similarity to the beta defensins but is now also recognized as a key iron regulatory hormone (4). Hepcidin is mainly produced by the liver in conditions of high iron, infection or inflammation. Hepcidin controls plasma iron levels by binding to ferroportin (FPN), the only known iron exporter, and inducing its degradation (5). Patients with iron overload are well known to be associated with a predisposition to a variety of infections. Hepcidin contributes to innate immunity by decreasing plasma iron levels providing an iron-restricted internal milieu inhospitable to microbes (6).

Besides the liver, an increasing number of studies showed that hepcidin is also expressed in other tissues (7-10). We previously demonstrated that hepatic hepcidin is sufficient to ensure systemic iron homeostasis in physiological conditions (11) suggesting that production of hepcidin by other tissues may have local roles. It may have a role at the site of infections and/or in poorly perfused tissues, inaccessible by systemic hepcidin from the circulation. The putative expression and local role of hepcidin in the skin, major site of AMP production are

not known. We have employed our recently generated mouse model, in which the hepcidin gene can be spatiotemporally inactivated, to explore the putative expression and role of hepcidin in the skin in the context of GAS infection.

Results and discussion

We examined hepcidin expression on skin biopsies derived from patients suffering from GAS NF (detailed in **Supplementary table 1**). Hepcidin staining of human liver tissue sections was used as a positive control (**Supplementary Figure 1**). Hepcidin expression was higher and more widespread in the skin of NF patients than in the skin of a healthy subject, especially in keratinocytes, the predominant cell type in the epidermis (**Figure 1A**). Hepcidin mRNA expression was induced (**Figure 1B)** in a human 3D organotypic skin model (**Supplementary Figure 2**) as a direct consequence of GAS infection. To investigate the role of hepcidin in the development of NF, we used an established model of necrotizing soft tissue infection (12, 13) where a strain of GAS, isolated from a patient with NF (14) is introduced subcutaneously into a shaved area on the flank of mice. Compared to skin biopsies of healthy mice, hepcidin expression was induced in the skin of infected mice (**Figure 1C**) and clearly detected in the keratinocytes as visualized by the Keratin 14 (K14) staining (**Figure 1D**).

To probe the functional significance of keratinocyte-derived hepcidin *in vivo*, we developed a mouse model of keratinocyte-specific hepcidin deficiency (*Hamp1*Δ^{ker}) by crossing *Hamp1*$^{lox/lox}$ mice with K14^{cre+} mice (**Figure 1E)**. We observed an efficient truncation of the floxed *Hamp1* allele in the epidermis of the *Hamp1*Δ^{ker} mice but not in the *Hamp1*$^{lox/lox}$ mice or K14-cre+ mice (**Supplementary Figure 3**). Systemic iron parameters were unchanged between *Hamp1*$^{lox/lox}$ and *Hamp1*Δ^{ker} mice (**Figure 1F**), in agreement with our previous study (11) suggesting that hepcidin production by extra-hepatic tissues does not contribute to systemic iron homeostasis. Iron levels were also similar in the skin of *Hamp1*Δ^{ker} and *Hamp1*$^{lox/lox}$ mice (**Figure 1F**).

These mice were infected with GAS in the NF model (14). Keratinocyte hepcidin staining was not detectable in the *Hamp1*Δ^{ker} mice (**Supplementary Figure 4**) confirming that the

stained hepcidin peptide is of skin but not of liver origin. Four days post-infection, *Hamp1*Δ^{ker} mice had a significantly higher number of bacteria than the *Hamp1*$^{lox/lox}$ littermates at the lesion site (10^6 vs 10^5 CFU/mg) but also in the blood (10^4 vs 9 x 10^2 CFU/ml) and in the spleen (5 x 10^4 vs 38 CFU/g) (**Figure 1G**). *Hamp1*Δ^{ker} mice also lost more weight than the *Hamp1*$^{lox/lox}$ mice, further underlining the higher morbidity in these mice (**Figure 1H**). These data indicate that keratinocyte production of hepcidin is important in limiting the ability of GAS to replicate within the necrotic skin tissues and to disseminate from the initial focus of infection into the bloodstream and systemic organs.

To investigate the mechanisms by which hepcidin protected against the spread of GAS infection, we first determined the putative bacteriostatic and bactericidal effects of hepcidin against GAS *in vitro*. While the well-known antimicrobial peptide LL-37 demonstrated bacteriostatic activities against GAS (**Figures 2A)**, hepcidin had neither bactericidal (**Figures 2A)** nor bacteriostatic activities (**Figures 2B)**. Moreover, primary keratinocytes derived from *Hamp1*$^{lox/lox}$ and *Hamp1*Δ^{ker} mice displayed the same bactericidal activity against this pathogen (**Figure 2C**). We therefore ruled out a direct antimicrobial effect of hepcidin on these bacteria.

AMPs have been reported to have pleiotropic effects and influence host's inflammatory responses during infection (15). We therefore asked whether hepcidin could have an immunomodulatory role in keratinocytes. For this purpose, we performed a cytoplex on the supernatant of murine primary keratinocytes incubated with 0.36 μM and 3.6 μM synthetic hepcidin. Interestingly, hepcidin induced a dose-dependent increase of the key neutrophil chemokine CXCL1 but not of the other inflammatory cytokines we tested (**Figure 2D**). The capacity of mouse hepcidin to induce CXCL1 in primary keratinocytes was confirmed by ELISA (**Supplementary Figure 5**) as well as the capacity of human hepcidin to induce the

production of IL-8, the human functional homolog of CXCL1 in the human HaCat keratinocyte cell line and in a human 3D organotypic skin model (**Figure 2E**).

The cognate receptor of hepcidin is the iron exporter FPN, questioning the role of FPN/iron in the induction of CXCL1 by hepcidin. The stimulatory effect of hepcidin on CXCL1 was reduced by the addition of a drug preventing the interaction of hepcidin with the iron exporter FPN (16) (**Figure 2F**). These data suggest that hepcidin, in primary keratinocytes, induces CXCL1 through a FPN dependent pathway. Binding of hepcidin to FPN is well known to induce its internalization and degradation resulting in an increase of intracellular iron (5). In corroboration with the action of hepcidin on FPN, incubation of primary keratinocytes with iron stimulated CXCL1 production (**Figure 2G**).

In agreement with the *in vitro* results showing that hepcidin stimulates CXCL1 production in primary keratinocytes, the *in vivo* keratinocyte CXCL1 production in response to GAS infection was lower in *Hamp1*Δ^{ker} mice than in *Hamp1*$^{lox/lox}$ littermates, as shown by IHC (**Figure 3A**) and ELISA (**Figure 3B**) on skin biopsies. As a consequence of the lower CXCL1 production, less neutrophil recruitment was observed in the skin of *Hamp1*Δ^{ker} mice compared to that of control littermates, as shown by IHC (**Figure 3C**) and by cytometry analysis (**Figure 3D**). This defect in the ability of keratinocyte-derived hepcidin to recruit neutrophils at the site of infection translated into a decrease in the necrotic skin lesion size of the *Hamp1*Δ^{ker} mice as compared to controls (**Figure 3E**). Subcutaneous injection of CXCL1 into GAS-infected *Hamp1*Δ^{ker} mice (**Figure 3F**) significantly decreased the number of bacteria even below to that found in the lesions of *Hamp1*$^{lox/lox}$ mice (**Figure 3G**). These results strongly suggest that the lack of CXCL1 production in *Hamp1*Δ^{ker} mice was responsible for their susceptibility to GAS infection. Altogether, these results suggest that

hepcidin is critical for regulating CXCL1 production in keratinocytes and that it may tune the magnitude of the neutrophil recruitment in the immune response.

We next investigated the possible advantages of indirect production of CXCL1 through hepcidin during GAS infection. GAS is equipped with a quantity of neutrophil resistance factors allowing the pathogen to uniquely counteract each anti-bacterial strategy of neutrophils (3). One of the principal mechanisms of GAS-immune escape is the production of surface-associated serine proteases by GAS, such as SpyCEP (also designated ScpC), that cleaves human IL-8/mouse CXCL1 to suppress chemokine-mediated neutrophil recruitment (17) or SpeB, which allows GAS to translocate across the epithelial barrier by degrading several host plasma and matrix proteins (18). To examine whether hepcidin was a target of SpyCEP or SpeB, synthetic hepcidin and CXCL1 (as a control) were incubated with purified SpyCEP, SpeB or PBS overnight. The digestion products were examined by mass spectrometry analyses. As shown by the MALDI spectrum (**Figure 4A**) CXCL1 was cleaved, as expected, into two fragments of 5.9 and 1.3 kDa. In contrast, hepcidin was not cleaved in presence of SpyCEP (**Figure 4A, bottom panel**) or SpeB (**Supplementary Figure 6**). This suggests that hepcidin could serve as a reservoir to maintain a steady-state level of CXCL1 in the context of infection. CXCL1 is phylogenetically ancient and is expressed in *Dictostelium discoideum,* while hepcidin-like peptides appeared more recently during evolution, for example in teleost fishes (**Supplementary Figure 7**). Considering the theory that host-pathogen interactions co-evolve, we could speculate that whereas GAS has already evolved to counteract the activity of CXCL1, it has not yet developed a virulence factor able to neutralize the activity of hepcidin. Because of hepcidin resistance to bacterial protease activities such as SpyCEP or SpeB, and in view of its unanticipated immunomodulatory role, we further asked whether local hepcidin injection could have a therapeutic effect on the systemic spread of bacteria in a NF model. Twenty-four hours after GAS infection, 1 μg of synthetic hepcidin or

PBS was subcutaneously injected at the bacterial inoculation site, followed by two injections of 500 ng of hepcidin or PBS for 2 consecutive days (**Figure 4B**). As expected, hepcidin-treated mice showed an increase in neutrophil recruitment (**Figure 4C**). In contrast to the PBS-treated mice, which exhibited systemic signs of infection including weight loss (**Figure 4D**), rough hair coat and hunched posture (data not shown), hepcidin-treated mice did not present any signs of systemic disease and accordingly recovered their initial weight. Remarkably, whereas all the control mice presented with systemic bacterial dissemination (as shown by the number of bacteria in the spleen), 7 out of the 9 hepcidin-treated mice showed absolutely no bacterial dissemination (**Figure 4E**). Hepcidin treatment did not prevent bacterial dissemination in CXCL1-/- mice (**Supplementary Figure 8**), showing that the therapeutic effect of hepcidin acted through CXCL1. Hepcidin thus demonstrated a therapeutic role in this mouse model of NF. These results suggest that hepcidin represents an alternative additional strategy for treating GAS-derived NF, and merits further investigation, especially in view of the increasing incidence of invasive GAS disease worldwide (19).

Altogether, we could speculate that skin hepcidin status (low vs high) may be a marker of sepsis development. Future studies should investigate whether skin hepcidin levels inversely correlate with the severity of sepsis development in NF patients.

In addition to its key role as an iron regulatory hormone produced by the liver, we have demonstrated here that epidermal hepcidin may also be an essential heretofore unrecognized component of the immune response to bacterial infection. Modulation of its expression may represent a novel therapeutic approach for necrotizing fasciitis patients.

METHODS

See supplementary information

Study approval

For human studies, informed consent to the protocol was obtained for all subjects and was approved by the Institutional Review Board and the regional ethics committee Paris IV (IRB 2016/40NICB), n° IRB 00003835. The collection of personal data was approved by the "Commission Nationale de l'Informatique et des Libertés".

The animal studies described here were reviewed and approved (Agreement n° CEEA34.CP.003.13) by the "Président du Comité d'Ethique pour l'Expérimentation Animale Paris Descartes" and are in accordance with the principles and guidelines established by the European Convention for the Protection of Laboratory Animals (Council of Europe, ETS 123, 1991).

AUTHOR CONTRIBUTIONS

M.M., S.L., S.C., S.M.S., and J.M.RR designed the experiments, carried out experiments and performed data analysis. A.F. AZ, C.H., C.G., N.O. and J-W.D. provided essential reagents and scientific advice. J.M.RR and C.P. designed experiments and supervised the project. C.P. wrote the manuscript.

ACKNOWLEDGEMENTS

This work was also supported by a funding from the European Research Council under the European Community's Seventh Framework Program (FP7/2011-2015 Grant agreement no 261296), the "Fondation pour la Recherche Médicale" (DEQ20160334903), the Laboratory of Excellence GR-Ex, reference ANR-11-LABX-0051, funded by the program "Investissements d'avenir" of the French National Research Agency, reference ANR-11-IDEX-0005-02 and the Swiss National Science Foundation grant 31003A_176252 to A.S.Z.

We are grateful to Sergio Lira for providing the CXCL1-/- mice. We thank the Henri Mondor Hospital Necrotizing Fasciitis Group (Sbidian Emilie, Bosc Romain, Chosidow Olivier, de Prost Nicolas, Tomberli Francoise, Woerther Paul Louis, Gomart Camille, Lepeule Raphael, Luciani Alain, Nakad Lionel, de Angelis Nicola, Champy Cecile), Antonin Weckel and Marthe Rizk for hepflul technical advice as well as Sophie Vaulont and Kurt Liittschwager for critical reading of the manuscript. We greatly acknowledge the Cochin 3P5 proteomics (François Guillonneau) and the HistIM, IMAG'IC and animal facilities.

REFERENCES

1. Hakkarainen TW, Kopari NM, Pham TN, and Evans HL. Necrotizing soft tissue infections: review and current concepts in treatment, systems of care, and outcomes. *Curr Probl Surg.* 2014;51(8):344-62.
2. Walker MJ, Barnett TC, McArthur JD, Cole JN, Gillen CM, Henningham A, Sriprakash KS, Sanderson-Smith ML, and Nizet V. Disease manifestations and pathogenic mechanisms of Group A Streptococcus. *Clin Microbiol Rev.* 2014;27(2):264-301.
3. Dohrmann S, Cole JN, and Nizet V. Conquering Neutrophils. *PLoS Pathog.* 2016;12(7):e1005682.
4. Krause A, Neitz S, Magert HJ, Schulz A, Forssmann WG, Schulz-Knappe P, and Adermann K. LEAP-1, a novel highly disulfide-bonded human peptide, exhibits antimicrobial activity. *FEBS Lett.* 2000;480(2-3):147-50.
5. Nemeth E, Tuttle MS, Powelson J, Vaughn MB, Donovan A, Ward DM, Ganz T, and Kaplan J. Hepcidin regulates cellular iron efflux by binding to ferroportin and inducing its internalization. *Science.* 2004;306(5704):2090-3.
6. Weiss G, Ganz T, and Goodnough LT. Anemia of inflammation. *Blood.* 2019;133(1):40-50.
7. Bekri S, Gual P, Anty R, Luciani N, Dahman M, Ramesh B, Iannelli A, Staccini-Myx A, Casanova D, Ben Amor I, et al. Increased adipose tissue expression of hepcidin in severe obesity is independent from diabetes and NASH. *Gastroenterology.* 2006;131(3):788-96.
8. Kulaksiz H, Theilig F, Bachmann S, Gehrke SG, Rost D, Janetzko A, Cetin Y, and Stremmel W. The iron-regulatory peptide hormone hepcidin: expression and cellular localization in the mammalian kidney. *J Endocrinol.* 2005;184(2):361-70.
9. Merle U, Fein E, Gehrke SG, Stremmel W, and Kulaksiz H. The iron regulatory peptide hepcidin is expressed in the heart and regulated by hypoxia and inflammation. *Endocrinology.* 2007;148(6):2663-8.
10. Peyssonnaux C, Zinkernagel AS, Datta V, Lauth X, Johnson RS, and Nizet V. TLR4-dependent hepcidin expression by myeloid cells in response to bacterial pathogens. *Blood.* 2006;107(9):3727-32.
11. Zumerle S, Mathieu JR, Delga S, Heinis M, Viatte L, Vaulont S, and Peyssonnaux C. Targeted disruption of hepcidin in the liver recapitulates the hemochromatotic phenotype. *Blood.* 2014;123(23):3646-50.
12. Datta V, Myskowski SM, Kwinn LA, Chiem DN, Varki N, Kansal RG, Kotb M, and Nizet V. Mutational analysis of the group A streptococcal operon encoding streptolysin S and its virulence role in invasive infection. *Mol Microbiol.* 2005;56(3):681-95.
13. Peyssonnaux C, Datta V, Cramer T, Doedens A, Theodorakis EA, Gallo RL, Hurtado-Ziola N, Nizet V, and Johnson RS. HIF-1alpha expression regulates the bactericidal capacity of phagocytes. *J Clin Invest.* 2005;115(7):1806-15.
14. Kansal RG, McGeer A, Low DE, Norrby-Teglund A, and Kotb M. Inverse relation between disease severity and expression of the streptococcal cysteine protease, SpeB, among clonal M1T1 isolates recovered from invasive group A streptococcal infection cases. *Infect Immun.* 2000;68(11):6362-9.
15. Nakatsuji T, and Gallo RL. Antimicrobial peptides: old molecules with new ideas. *J Invest Dermatol.* 2012;132(3 Pt 2):887-95.

16. Ross SL, Biswas K, Rottman J, Allen JR, Long J, Miranda LP, Winters A, and Arvedson TL. Identification of Antibody and Small Molecule Antagonists of Ferroportin-Hepcidin Interaction. *Front Pharmacol.* 2017;8(838.
17. Zinkernagel AS, Timmer AM, Pence MA, Locke JB, Buchanan JT, Turner CE, Mishalian I, Sriskandan S, Hanski E, and Nizet V. The IL-8 protease SpyCEP/ScpC of group A Streptococcus promotes resistance to neutrophil killing. *Cell Host Microbe.* 2008;4(2):170-8.
18. Nelson DC, Garbe J, and Collin M. Cysteine proteinase SpeB from Streptococcus pyogenes - a potent modifier of immunologically important host and bacterial proteins. *Biol Chem.* 2011;392(12):1077-88.
19. Sims Sanyahumbi A, Colquhoun S, Wyber R, and Carapetis JR. In: Ferretti JJ, Stevens DL, and Fischetti VA eds. *Streptococcus pyogenes : Basic Biology to Clinical Manifestations*. Oklahoma City (OK); 2016.

FIGURE LEGENDS

Figure 1. Keratinocyte hepcidin prevents bacterial systemic spread

Immunohistochemistry (IHC) with or without primary antibody detecting (**A**) hepcidin (in brown) on sections of cutaneous human biopsies of GAS NF patients and healthy control using PerkinElmer's LaminaTM multilabel slide scanner Panoramic Viewer software. (**B**) Q-PCR for hepcidin from GAS-infected human 3D organotypic skin equivalent model. N=4 per group. (**C**) Q-PCR for hepcidin in murine GAS-infected skin. N ≥ 3 per group. (**D**) Hepcidin (in blue) and K14 (in brown) IHC on cutaneous biopsies of WT mice challenged or not with GAS. Bars represent 100 μm. (5/0.4, Leica DMI3000B microscope, Leica DFC310FX camera [Leica LAS Core software]). (**E**) Generation of *Hamp1*Δ^{ker} mice. (**F**) Plasma iron, ferritin, transferrin and skin iron levels in *Hamp1*$^{lox/lox}$ and *Hamp1*Δ^{ker} mice. N ≥ 4 per group. (**G**) Bacterial count in skin, blood and spleen of *Hamp1*$^{lox/lox}$ and *Hamp1*Δ^{ker} mice four days after injection with GAS. N ≥ 10 per group. (**H**) Weight variation of *Hamp1*$^{lox/lox}$ and *Hamp1*Δ^{ker} mice during infection. N=10 per group. Statistical analysis was performed using a Mann Whitney test (B, C, F, G) or a two-way analysis of variance (ANOVA) followed by a Tukey test for weight kinetics (H).

Figure 2. Hepcidin promotes CXCL1 production by keratinocytes

(**A**) GAS killing kinetics with 32 μM of LL-37 and hepcidin. N=3 per group. Representative of 2 independent experiments. (**B**) GAS growth curve in the presence of pennicilin G, LL-37, hepcidin or PBS. N=3 per group. Representative of 2 independent experiments. (**C**) Bacterial recovering at 1h and 3h following incubation of log-phase GAS with murine primary keratinocytes (KC) from *Hamp1*$^{lox/lox}$ and *Hamp1*Δ^{ker} mice. Data are representative of two

independent experiments performed in triplicate. (**D**) Cytokines measured with the V-PLEX Proinflammatory Panel1 kit in the culture supernatant of murine primary keratinocytes stimulated for 1 or 3 h with hepcidin or PBS. N=3 per group. Representative of 3 independent experiments. (**E**) IL-8 ELISA on the culture supernatant of HaCat or a human 3D skin equivalent model stimulated with 3.6 μM hepcidin. N≥3 per group. (**F**) CXCL1 levels measured by ELISA in the culture supernatant of murine primary keratinocytes stimulated for 3 h with 3.6 μM hepcidin in presence of PBS or 100 μM FPN inhibitor (2D-014). N ≥ 3 per group. Representative of 3 independent experiments. (**G**) CXCL1 levels measured by ELISA on the culture supernatant of murine primary keratinocytes stimulated for 3 h with 500 μM Ferric Ammonium Citrate (FAC). N=3 per group. Representative of 3 independent experiments. Statistical analysis was performed using a two-way ANOVA followed by a Tukey test (A,B,D), unpaired Student's t-test (E, G) or a one-way ANOVA followed by a Tukey test (C,F).

Figure 3. Hepcidin is required for CXCL1 production and neutrophil recruitment

(**A**) Anti-CXCL1 or (**C**) anti polymorphonuclear leucocytes (PMN) immunostainings on skin of *Hamp1*$^{lox/lox}$ and *Hamp1*Δ^{ker} mice challenged with GAS. PerkinElmer's LaminaTM multilabel slide scanner Panoramic Viewer software. (**B**) CXCL1 ELISA on lysates from GAS-infected skin biopsies of *Hamp1*$^{lox/lox}$ (n=5) and *Hamp1*Δ^{ker} mice (n=6). (**D**) Neutrophil count from GAS-infected skin biopsies of *Hamp1*$^{lox/lox}$ (n=5) and *Hamp1*Δ^{ker} mice (n=4). (**E**) Area of necrotic ulcers in skin of *Hamp1*$^{lox/lox}$ and *Hamp1*Δ^{ker} mice during GAS infection. N=7 per group. (**F**) Scheme of the study protocol. (**G**) Bacterial count in the skin of *Hamp1*$^{lox/lox}$ and *Hamp1*Δ^{ker} mice injected daily with CXCL1 or PBS. N≥4 per group.

Statistical analysis was performed using a Student's t-test (B, D), a two-way ANOVA followed by a Tukey test (**E**) or a one-way ANOVA followed by a Tukey test (G).

Figure 4. Hepcidin is resistant to SpyCEP cleavage and has a therapeutic role in NF

(**A**) Mass spectroscopy analysis of CXCL1 or hepcidin incubated overnight with SpyCEP or PBS. Electrospray ionization generated a series of multiply charged ions (indicated as m/z; mass-to-charge ratio) from which the average molecular mass (m) of each was deduced. The blue arrows indicate uncleaved peptide peaks at 7.8 kDa (CXCL1) and 2.7 kDa (hepcidin). Red arrows show the cleavage products of CXCL1 with a small (1.3 kDa) and a big (5.9 kDa) fragment. (**B**) Therapeutic protocol. (**C**) Neutrophil count (three measurements per individual mouse were averaged). N=6 per group (**D**) Weight variation and (**E**) bacterial count in spleen of WT infected mice treated with PBS or hepcidin (n=9, red square) or PBS (n=9, black square) during 4 days. Statistical analysis was performed using a Student's t-test (C), a two-way ANOVA followed by a Tukey test (D) or a Mann Whitney test (E).

FIGURE 1

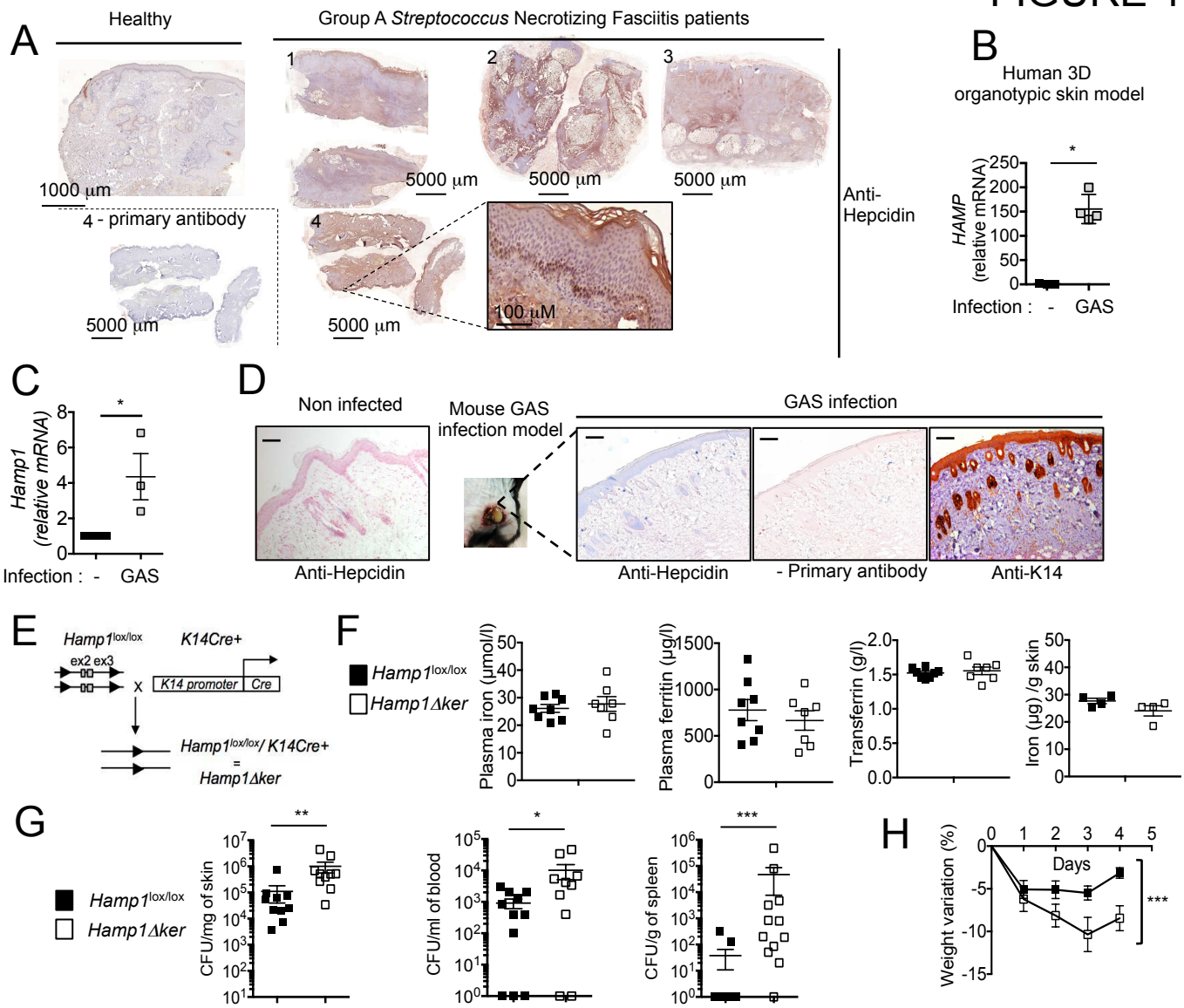

Figure 1. Keratinocyte hepcidin prevents bacterial systemic spread

Immunohistochemistry (IHC) with or without primary antibody detecting (**A**) hepcidin (in brown) on sections of cutaneous human biopsies of GAS NF patients and healthy control using PerkinElmer's LaminaTM multilabel slide scanner Panoramic Viewer software. (**B**) Q-PCR for hepcidin from GAS-infected human 3D organotypic skin equivalent model. N=4 per group. (**C**) Q-PCR for hepcidin in murine GAS-infected skin. N≥3 per group. (**D**) Hepcidin (in blue) and K14 (in brown) IHC on cutaneous biopsies of WT mice challenged or not with GAS. Bars represent 100 µm. (5/0.4, Leica DMI3000B microscope, Leica DFC310FX camera [Leica LAS Core software]). (**E**) Generation of *Hamp1*Δ^{ker}mice. (**F**) Plasma iron, ferritin, transferrin and skin iron levels in *Hamp1*$^{lox/lox}$ and *Hamp1*Δ^{ker} mice. N ≥ 4 per group. (**G**) Bacterial count in skin, blood and spleen of *Hamp1*$^{lox/lox}$ and *Hamp1*Δ^{ker}mice four days after injection with GAS. N ≥ 10 per group. (**H**) Weight variation of *Hamp1*$^{lox/lox}$ and *Hamp1*Δ^{ker} mice during infection. N=10 per group. Statistical analysis was performed using a Mann Whitney test (B, C, F, G) or a two-way analysis of variance (ANOVA) followed by a Tukey test for weight kinetics (H).

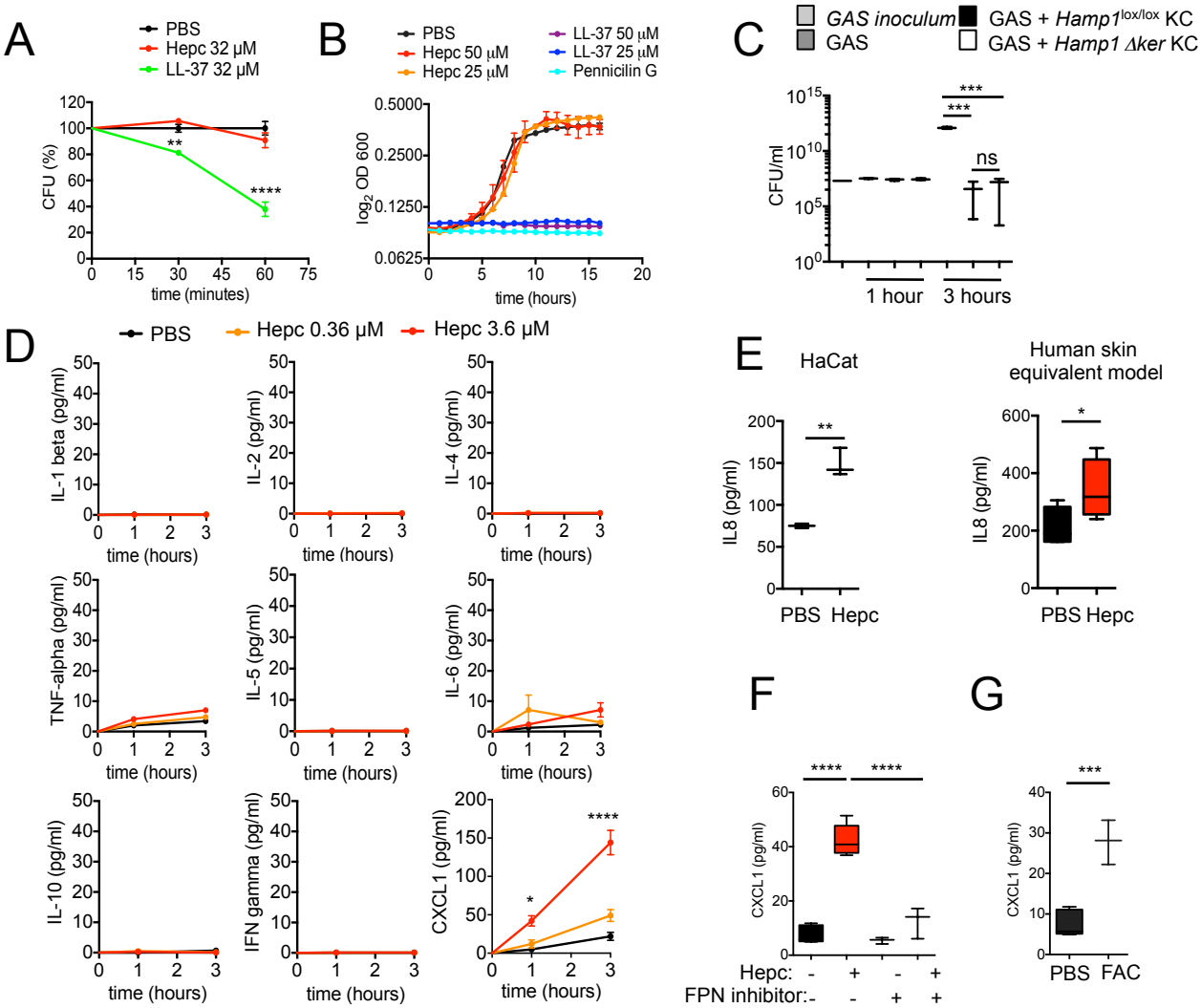

Figure 2. Hepcidin promotes CXCL1 production by keratinocytes

(**A**) GAS killing kinetics with 32 µM of LL-37 and hepcidin. N=3 per group. Representative of 2 independent experiments. (**B**) GAS growth curve in the presence of pennicilin G, LL-37, hepcidin or PBS. N=3 per group. Representative of 2 independent experiments. (**C**) Bacterial recovering at 1h and 3h following incubation of log-phase GAS with murine primary keratinocytes (KC) from *Hamp1*$^{lox/lox}$ and *Hamp1*Δ^{ker} mice. Data are representative of two independent experiments performed in triplicate. (**D**) Cytokines measured with the V-PLEX Proinflammatory Panel1 kit in the culture supernatant of murine primary keratinocytes stimulated for 1 or 3 h with hepcidin or PBS. N=3 per group. Representative of 3 independent experiments. (**E**) IL-8 ELISA on the culture supernatant of HaCat or a human 3D skin equivalent model stimulated with 3.6 µM hepcidin. N≥3 per group. (**F**) CXCL1 levels measured by ELISA in the culture supernatant of murine primary keratinocytes stimulated for 3 h with 3.6 µM hepcidin in presence of PBS or 100 µM FPN inhibitor (2D-014). N≥ 3 per group. Representative of 3 independent experiments. (**G**) CXCL1 levels measured by ELISA on the culture supernatant of murine primary keratinocytes stimulated for 3 h with 500 µM Ferric Ammonium Citrate (FAC). N≥3 per group. Representative of 3 independent experiments. Statistical analysis was performed using a two-way ANOVA followed by a Tukey test (A,B,D), unpaired Student's t-test (E, G) or a one-way ANOVA followed by a Tukey test (C,F).

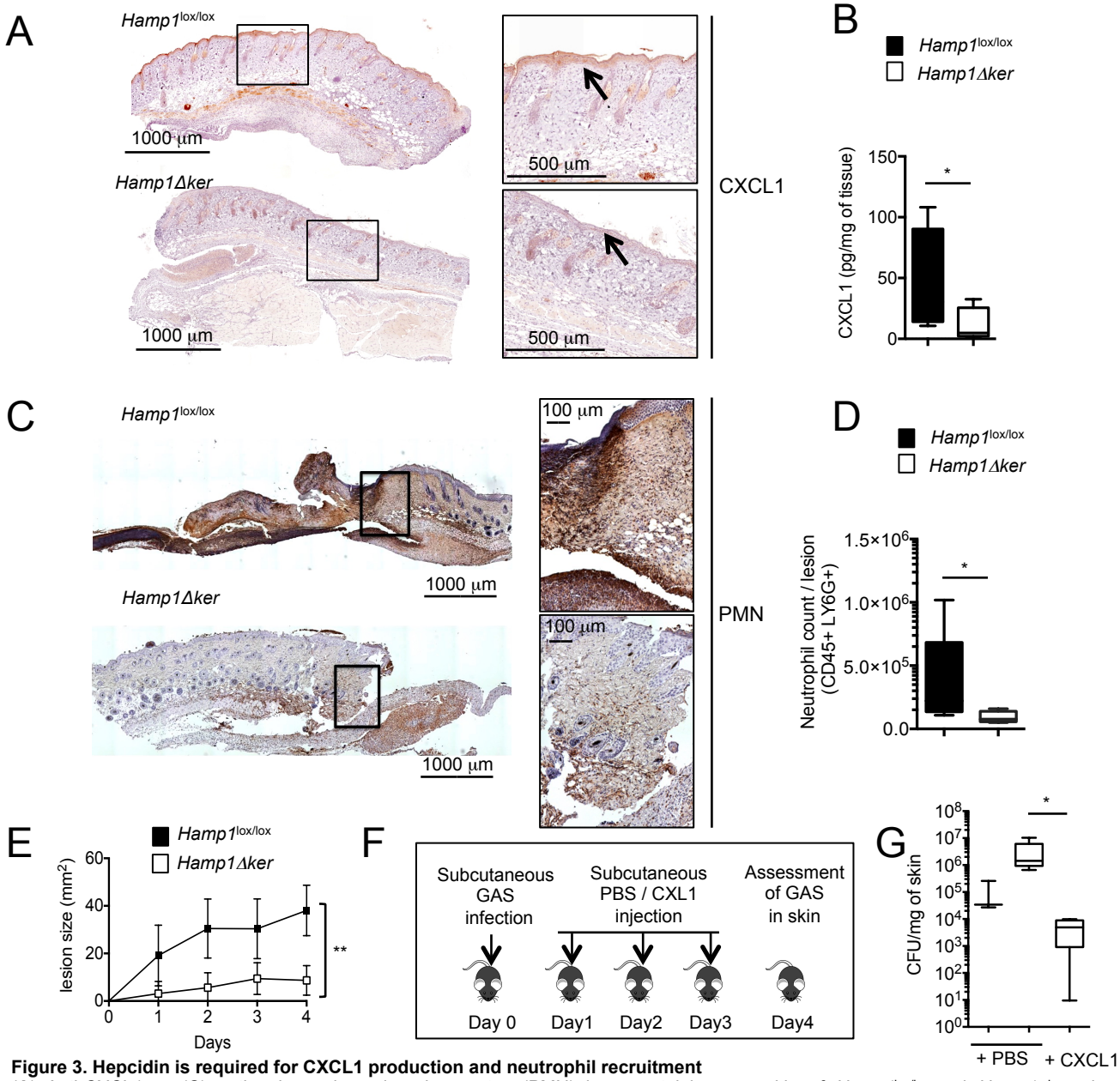

Figure 3. Hepcidin is required for CXCL1 production and neutrophil recruitment

(**A**) Anti-CXCL1 or (**C**) anti polymorphonuclear leucocytes (PMN) immunostainings on skin of *Hamp1*$^{lox/lox}$ and *Hamp1*Δ^{ker} mice challenged with GAS. PerkinElmer's LaminaTM multilabel slide scanner Panoramic Viewer software. (**B**) CXCL1 ELISA on lysates from GAS-infected skin biopsies of *Hamp1*$^{lox/lox}$ (n=5) and *Hamp1*Δ^{ker} mice (n=6). (**D**) Neutrophil count from GAS-infected skin biopsies of *Hamp1*$^{lox/lox}$ (n=5) and *Hamp1*Δ^{ker} mice (n=4). (**E**) Area of necrotic ulcers in skin of *Hamp1*$^{lox/lox}$ and *Hamp1*Δ^{ker} mice during GAS infection. N=7 per group. (**F**) Scheme of the study protocol. (**G**) Bacterial count in the skin of *Hamp1*$^{lox/lox}$ and *Hamp1*Δ^{ker} mice injected daily with CXCL1 or PBS. N≥4 per group. Statistical analysis was performed using a Student's t-test (B, D), a two-way ANOVA followed by a Tukey test (E) or a one-way ANOVA followed by a Tukey test (G).

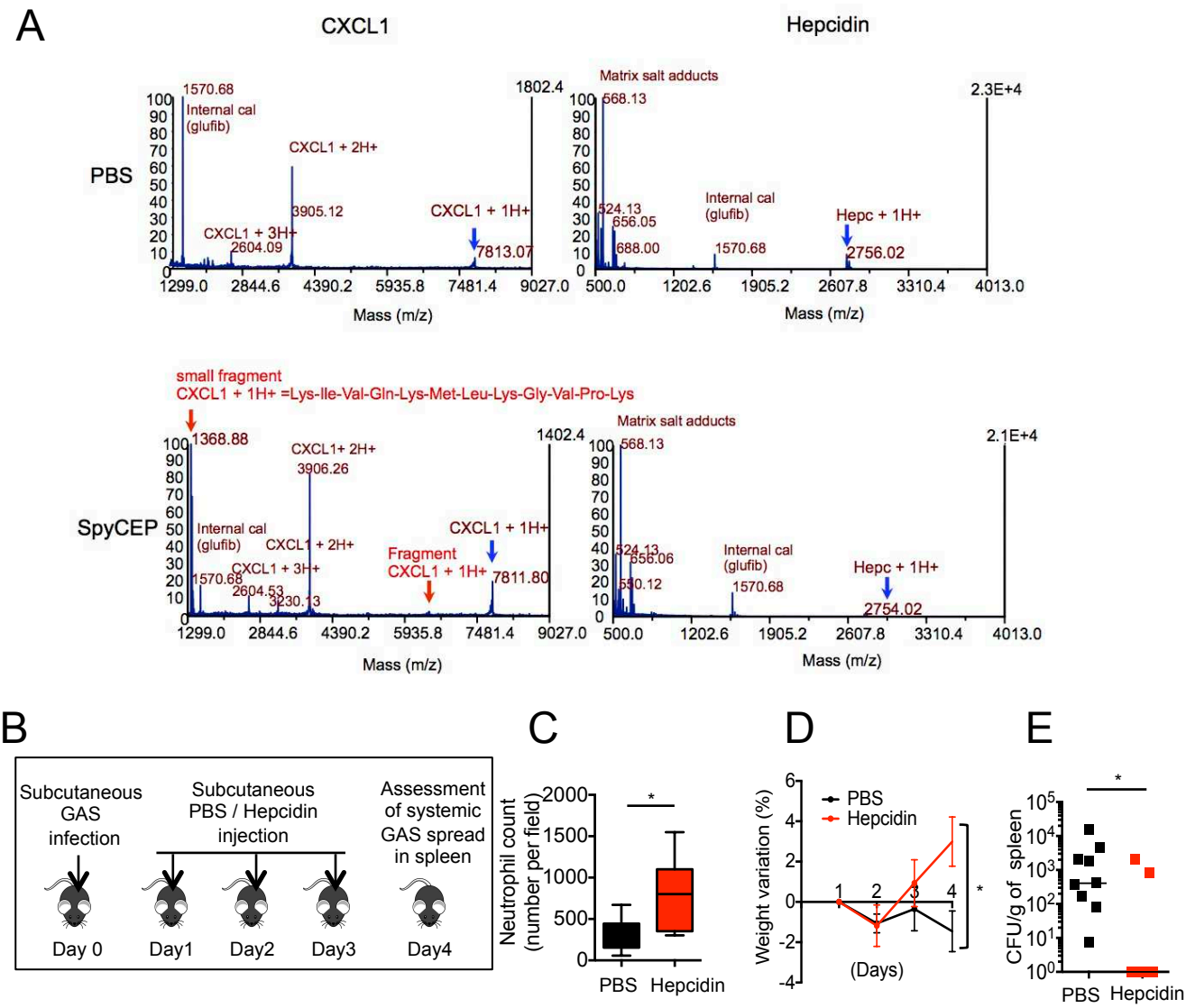

Figure 4. Hepcidin is resistant to SpyCEP cleavage and has a therapeutic role in NF

(**A**) Mass spectroscopy analysis of CXCL1 or hepcidin incubated overnight with SpyCEP or PBS. Electrospray ionization generated a series of multiply charged ions (indicated as m/z; mass-to-charge ratio) from which the average molecular mass (m) of each was deduced. The blue arrows indicate uncleaved peptide peaks at 7.8 kDa (CXCL1) and 2.7 kDa (hepcidin). Red arrows show the cleavage products of CXCL1 with a small (1.3 kDa) and a big (5.9 kDa) fragment. (**B**) Therapeutic protocol. (**C**) Neutrophil count (three measurements per individual mouse were averaged). N=6 per group (**D**) Weight variation and (**E**) bacterial count in spleen of WT infected mice treated with PBS or hepcidin (n=9, red square) or PBS (n=9, black square) during 4 days. Statistical analysis was performed using a Student's t-test (C), a two-way ANOVA followed by a Tukey test (D) or a Mann Whitney test (E).